All-angle negative refraction in a three-dimensionally periodic photonic crystal

Chiyan Luo,[a] Steven G. Johnson, and J. D. Joannopoulos
Department of Physics and Center for Materials Science and Engineering, Massachusetts Institute of Technology, Cambridge, Massachusetts 02139

(Received 9 May 2002; accepted for publication 29 July 2002)

We introduce a photonic crystal that has a large range of effective negative refractive index in three dimensions (3D) and demonstrate its negative-refraction property by numerical simulations. With slight modifications, our design is also amenable to layer-by-layer fabrication. This work should enable experimental observation of negative refraction and related phenomena in 3D at optical frequencies. © *2002 American Institute of Physics.* [DOI: 10.1063/1.1508807]

Negative refraction of electromagnetic waves was first predicted in materials with simultaneously negative permeability and permittivity by Veselago in the 1960s.[1] Recently, it was proposed that negative refraction could be observed in artificial materials, such as left-handed materials at microwave lengthscales[2–6] and photonic crystals at optical frequencies,[7–9] with either negative[2–6,8] or positive[9] index of refraction. However, most of these results were obtained only for two-dimensionally (2D) periodic structures where negative refraction happens only for light traveling in the 2D plane. This puts severe limitations on realistic applications of this principle, superlenses[1,10] being an example. It is thus important to design a three-dimensionally periodic photonic crystal that enables fully three-dimensional (3D) negative refraction. This is a nontrivial problem since the bandstructure of 3D photonic crystals is considerably more complicated than that of their 2D counterparts. In particular, the photonic modes along an arbitrary direction are no longer polarized, the photonic band gaps are rarer, and there is usually more than one band at a single frequency. As a result, several outgoing beams can emerge from a single refraction process, and the old description in 2D in terms of an effective negative refractive index becomes difficult.

The subject of the present paper is to demonstrate a 3D photonic crystal with a large frequency range in which the effective negative-index concept is still valid. In particular, we study the possibility of all-angle negative refraction (AANR), i.e., negative refraction for beams of *all* incident angles from air. This is the case of practical interest because AANR precludes modes with very small group velocities, which are close to band edges and are generally difficult to couple to from an external planewave. Moreover, AANR also eliminates the effect of total *external* reflection, which exists for some angles if the absolute value of the effective index is less than unity and might be undesirable in some applications. To realize AANR, sufficient criteria are that the frequency range be near a *negative* ''photonic-mass'' region in the band structure and below the diffraction threshold, and that the photonic-crystal constant-frequency contour be *all-convex* and *larger* than that of air.[9] Clearly, this is only possible in the first few bands. In addition, as described later in this letter, above the first two bands care must be taken to ensure that the symmetry of the photonic modes allows good coupling from external planewaves.

The geometric lattice of the 3D photonic crystal can be determined from the following intuitive argument. In the periodic zone scheme, the constant-frequency contour for the first few bands of the photonic crystal can be constructed by joining all the spherical contours of an effective *uniform* medium that are centered on the reciprocal lattice sites and rounding the sharp parts of the joint surface across Brillouin zone boundaries.[8,11] For a given Brillouin zone *corner C*, we expect that the more neighboring reciprocal-lattice sites C has, the stronger the resulting rounding effect and the easier it is for the constant-frequency contours to become all-convex around C. Thus, a rough rule to choose the geometric lattice for AANR is just to maximize the number N of C's nearest-neighbor reciprocal-lattice sites. If AANR is to be realized in the fundamental (i.e., the first two) bands, then C is a corner of the first Brillouin zone. In this case, a simple-cubic (SC) *reciprocal* lattice with $N=8$ should be used, resulting in a SC photonic crystal with (111) surface termination. If AANR is to be realized in the bands after folding once, then C is a corner of the *second* Brillouin zone, which in most lattices is just Γ after translation of a reciprocal-lattice vector. This is the usual effective negative-index situation, and the face-centered cubic (fcc) *reciprocal* lattice which has $N=12$ should be chosen, giving a body-centered cubic (bcc) structure in real space. We will focus on the case of $N=12$, and will demonstrate, through band-structure calculations and numerical simulations, that a bcc photonic crystal with (101) surface termination is a good candidate for achieving AANR.

The structure we are proposing consists of a bcc lattice of air cubes in dielectric $\epsilon=18.0$ (e.g., Ge at $\lambda=1.55\mu$m). The sides of the air cubes have length $0.75a$ and are parallel to the sides of the conventional bcc cell, whose length is taken to be a. The band structure of this photonic crystal is shown in Fig. 1. Marked out in shaded regions on the band structure is a large AANR frequency range of 8.2%, from $0.375(2\pi c/a)$ to $0.407(2\pi c/a)$ in the third band. Within this frequency range, the constant-frequency contour of the photonic crystal forms a single all-convex surface which is larger than that of air. In particular, we show the contour at

[a]Electronic mail: chiyan@mit.edu

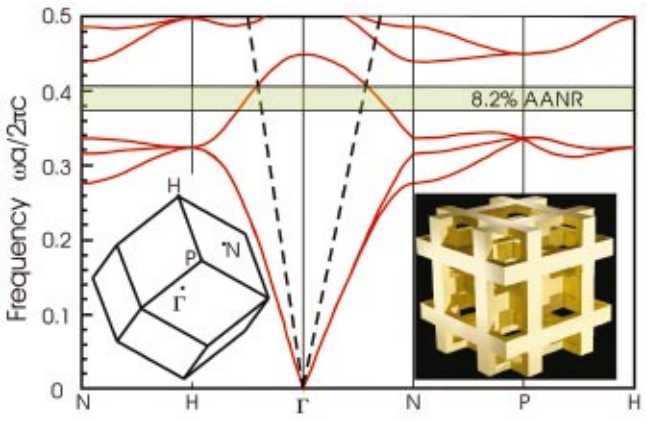

FIG. 1. (Color) Band structure (red) of a bcc lattice of air cubes in dielectric $\epsilon=18$. The cubes have sides $0.75a$ and are oriented with sides parallel to those of the conventional bcc cell. In the shaded AANR frequency range (green), the photonic crystal exhibits negative refraction for incoming radiation of all angles. The dashed lines are light lines along Γ H and Γ N. Insets are the shape and special symmetry vertices of the first Brillouin zone and a computer rendering of the actual crystal.

$\omega=0.407(2\pi c/a)$ in Fig. 2, which is nearly spherical with radius ω/c. In terms of the effective refractive index n_{eff} in 3D, the photonic crystal at this frequency may be regarded as $n_{\text{eff}}\approx-1$, and the AANR frequency region corresponds to $n_{\text{eff}}\leqslant-1$. Of course, $-1<n_{\text{eff}}<0$ also holds true for the frequency region above $0.407(2\pi c/a)$ and below the fourth band. We also note that a complete photonic band gap between the third and the fourth bands can result if larger cubes are used; however, a complete photonic band gap is not necessary in our case.

Because there is only one band in the frequency range of effective negative index, we expect that the negative-refraction phenomena in this frequency range will be strongly polarization dependent. In particular, the (001) surface should *not* be used for negative refraction. This is because, along the (001) direction, the two degenerate polarizations of normal-incidence radiation and the singly-degenerate photonic crystal mode belong to different irreducible representations of the surface symmetry group. As a consequence, they do not couple to each other. On the

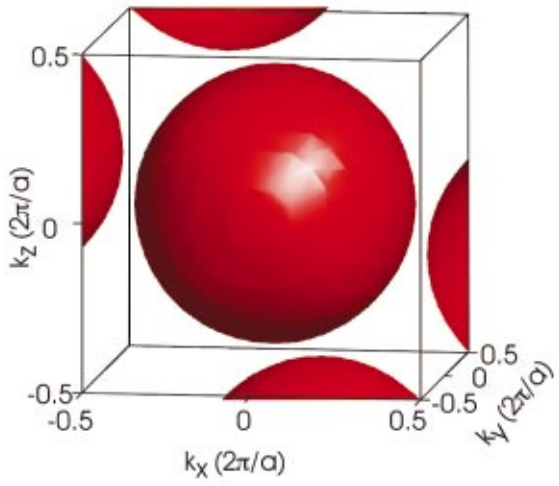

FIG. 2. (Color) The constant-frequency contour of the crystal in Fig. 1 at $\omega=0.407(2\pi c/a)$ in a repeated zone scheme.

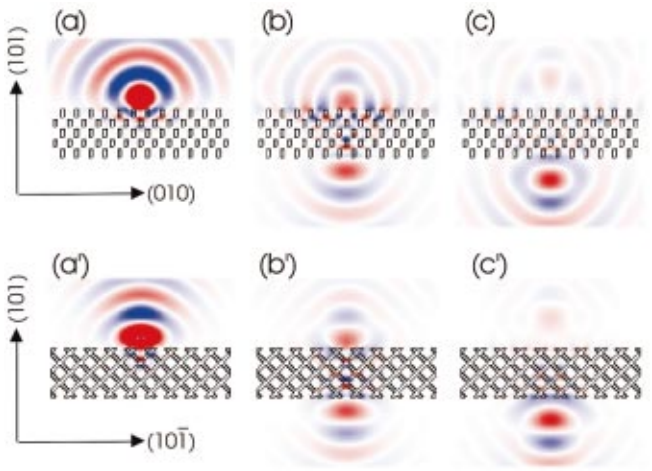

FIG. 3. (Color) 2D snapshots of electric field along $(10\bar{1})$ during an FDTD simulation of negative refraction of a $(10\bar{1})$-pointing pulsed dipole source, using an amplified color table that exhibits the field in most of the computational cell. Red, white, and blue stand for positive, zero, and negative of the field value, respectively. (a), (b), and (c) are slices through the (010)-(101) plane and (a'), (b'), and (c') are slices through the (101)-(101) plane, both planes containing the dipole. (a) and (a') are taken when the dipole reaches its peak, (b) and (b') are at an intermediate timestep, and (c) and (c') are at the instant when the image roughly reaches its peak. Black contours outline the dielectric structure.

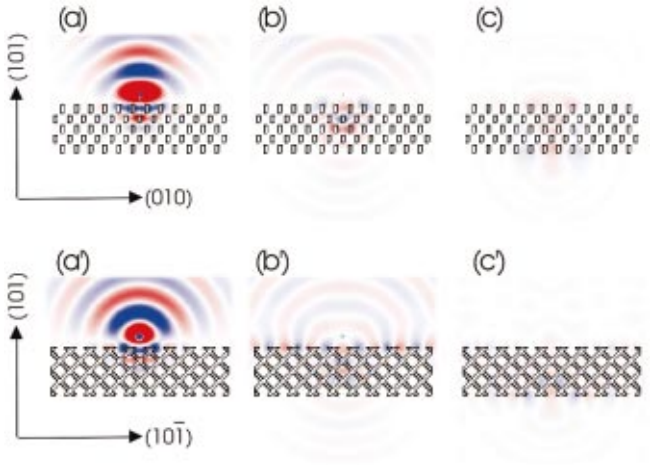

FIG. 4. (Color) 2D snapshots of electric field along (010) during an FDTD simulation similar to that in Fig. 3 with the dipole source pointing toward (010). The color table, slice positions and snapshot instants are the same as those in Fig. 3.

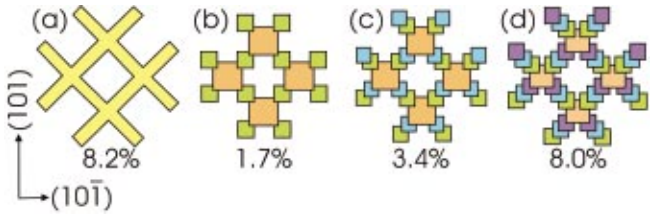

FIG. 5. (Color) Side cross sections of the original and modified designs. (a) Original design of Fig. 1. (b)–(d) Designs that approximate (a) using several layers amenable to lithographic etching along (101). For clarity, the layers are assigned different colors but are made of the same high-index material. Note that to make the layers overlap etching is also required at the joints. The numbers are the AANR size achievable in each case.

other hand, if we consider the (101) direction, then the two polarizations are no longer degenerate, and one of them can couple to the photonic crystal mode. In this case, it is waves polarized along $(10\bar{1})$ that couple strongly to the photonic crystal mode. For the other polarization along (010), the coupling efficiency is 0 at normal incidence and very weak at nonzero incident angles. In summary, the negative-index behavior in our photonic crystal applies most effectively on the (101) surface for the $(10\bar{1})$ polarization. This dependence of coupling efficiency on surface termination and polarization direction is an important difference between our photonic crystal and an *isotropic*, *uniform* medium with a negative refractive index.

To demonstrate AANR in 3D and to illustrate the polarization dependence, we have performed 3D finite-difference time-domain (FDTD) numerical simulations with perfectly matched layer boundary regions[12,13] on a finite slab of our photonic crystal with (101) surface termination to realize superlensing. We excite a pulsed point-dipole source of center frequency $0.39(2\pi c/a)$ at a distance of $0.72a$ above the top surface of the photonic crystal, and observe the radiation field distribution as a function of time. In Fig. 3 we show the results when the dipole is pointing along the $(10\bar{1})$ direction. The simulation shows that a significant fraction (roughly 27% out of a possible 50%) of the total dipole radiation transmits through the photonic crystal slab and become refocused into a wavelength-sized image below the slab. Since the focusing effect can be observed from both planes, it clearly demonstrates the fully 3D negative-refraction effect. There are some reflections from our photonic crystal visible here, but this is largely due to finite bandwidth of the pulse source. In principle, an appropriate width of the photonic crystal slab can always be chosen to minimize reflections at one frequency. On the other hand, if the dipole is pointing along (010), then most of the radiation fields are reflected. This is shown in Fig. 4. The fraction of power transmitted through the structure is only 3.6% (instead of 27%) and is from other frequency components outside the desired band. Thus, for this polarization the negative refraction effect is rather weak. This strong polarization dependence can be exploited for polarization-sensitive applications.

Although we have used $\epsilon=18$ for the high index material in these calculations, in practice other materials can also be used. In particular, Si with $\epsilon=12$ at 1.55μm yields an AANR frequency range of 3.2% around $0.464(2\pi c/a)$. Of course, low index material can be used in place of air if the overall dielectric contrast is large enough. At present, the fabrication of our photonic crystal in the original design at submicron lengthscales is still a challenging task because this design is not in a simple-layered form amenable to lithographic etching in the (101) direction. A simple modification for practical fabrication would be to employ the ''stair'' structures, as shown in Fig. 5. Here, several slightly-overlapping layers are used to approximate the original design. The whole structure can then be constructed by etching on the high-index material layer by layer, in a manner similar to those presented in Ref. 14. Our calculations indicate that AANR can be still achieved in all of these approximate designs, and particularly the design in Fig. 5(d) can reproduce roughly the same AANR frequency range size as in the original design. Thus, it should also be possible experimentally to verify the 3D AANR effects introduced in this letter.

This work is supported in part by the MRSEC program of the National Science Foundation under Grant No. DMR-9400334 and the DoD/ONR MURI Grant No. N00014-01-1-0803.

[1] V. G. Veselago, Sov. Phys. Usp. **10**, 509 (1968).
[2] J. B. Pendry, A. J. Holden, W. J. Stewart, and I. Youngs, Phys. Rev. Lett. **76**, 4773 (1996).
[3] J. B. Pendry, A. J. Holden, D. J. Robbins, and W. J. Stewart, IEEE Trans. Microwave Theory Tech. **47**, 2075 (1999).
[4] D. R. Smith, W. J. Padilla, D. C. View, S. C. Nemat-Nasser, and S. Schultz, Phys. Rev. Lett. **84**, 4184 (2000).
[5] R. A. Shelby, D. R. Smith, and S. Schultz, Science **292**, 77 (2001).
[6] R. A. Shelby, D. R. Smith, S. C. Nemat-Nasser, and S. Schultz, Appl. Phys. Lett. **78**, 489 (2001).
[7] H. Kosaka, T. Kawashima, A. Tomita, M. Notomi, T. Tamamura, T. Sato, and S. Kawakami, Phys. Rev. B **58**, 10096 (1998).
[8] M. Notomi, Phys. Rev. B **62**, 10696 (2000).
[9] C. Luo, S. G. Johnson, J. D. Joannopoulos, and J. B. Pendry, Phys. Rev. B **65**, 201104 (R) (2002).
[10] J. B. Pendry, Phys. Rev. Lett. **85**, 3966 (2000).
[11] N. W. Ashcroft and N. D. Mermin, *Solid State Physics* (Saunders College, Philadelphia, 1976).
[12] J.-P. Berenger, J. Comput. Phys. **114**, 185 (1994).
[13] D. C. Katz, E. T. Thiele, and A. Taflove, IEEE Microwave Guid. Wave Lett. **4**, 268 (1994).
[14] S. G. Johnson and J. D. Joannopoulos, Appl. Phys. Lett. **77**, 3490 (2000).